9TH INTERNATIONAL CONFERENCE ON MODIFICATION OF MATERIALS WITH PARTICLE BEAMS AND PLASMA FLOWS
Tomsk, Russia, 21–26 September 2008

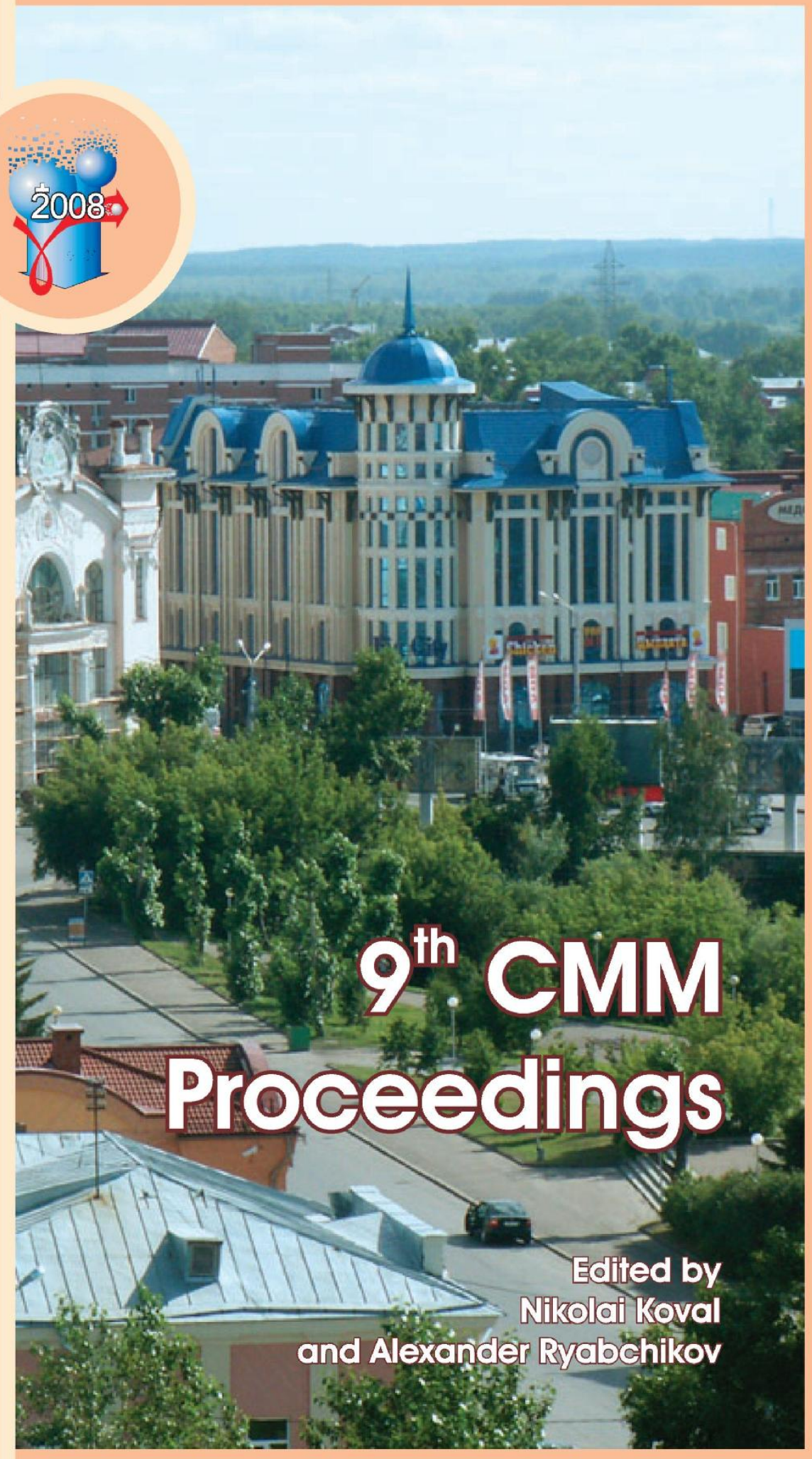

9th CMM Proceedings

Edited by
Nikolai Koval
and Alexander Ryabchikov

9th International Conference on Modification of Materials with Particle Beams and Plasma Flows

is HOSTED by

Institute of High Current Electronics SB RAS

Nuclear Physics Institute of Tomsk Polytechnic University

High Voltage Research Institute of Tomsk Polytechnic University

Tomsk Polytechnic University

and SPONSORED by

RUSSIAN ACADEMY OF SCIENCES

Russian Foundation for Basic Research

Tomsk Polytechnic University

9th International Conferenceon Modification of Materials with Particle Beams and Plasma Flows: Proceedings. Tomsk: Publishing house of the IAO SB RAS, 2008. 734 pp.

ISBN 978-5-94458-090-0

The Influence of Intense Pulsed Ion Beams and Compression Plasma Flows Treatment on Phase Composition and Mechanical Properties of WC–TiC–Co Hard Alloy Surface Layer

V.V. Uglov, G.E. Remnev*, A.K. Kuleshov, N.N. Cherenda, V.M. Astashinski**, and M.S. Saltymakov*

Belarusian State University, 4, Nezavizimosti, Minsk, 220030, Belarus
Phone: +8(375-17) 209-55-12, E-mail: uglov@bsu.by
**Nuclear Physics Institute, 2a, Lenin ave., Tomsk, 634050, Russia*
E-mail: remnev@hvd.tpu.ru
***B.I. Stepanov Institute of Physics of Belarus National Academy of Sciences, 68, Nezavisimosti, Minsk, 220072, Belarus*
Phone: +8(375-17) 284-10-65, E-mail: ast@imaph.bas-net.by

Abstract – The intense pulsed ion beams and compression plasma flows treatment of WC–TiC–Co hard alloy forms fused surface layer of solid solution $(W_x, Ti_{1-x})C$ supersaturated by tungsten. The thickness and degree of its supersaturation by tungsten increases with the amplify of energy density during impulse. Hardness of the surface layer containing supersaturated solid solution $(W_x, Ti_{1-x})C$ in some micron in the thickness exceeds in 2 times the hardness of untreated hard alloy T15K6.

1. Introduction

Treatment of materials by pulse high-power ion, electron, laser and plasma beams is a prospective method of hard alloys tools wear-resistance increase [1–6]. The main reason of hard alloys hardening is fast melting with the following crystallization under the conditions of high cooling rate (~10^7 K/s). Hardened zone consisting of a fused layer with the modified phase composition, dispersed structure and high density of defects can be formed on the tool leading edge depending on the pulse duration and beam power. Surface layer of hard alloy tools modified in such a way possesses high hardness and wear-resistance. Investigation of the changes of phase and element composition, microstructure and hardness along the depth of WC-TiC-Co hard alloy (T15K6) after treatment by high intensity pulse ion beam (HIPIB) and compression plasma flow (CPF) was the main aim of this work. The energy density during CPF treatment was either similar to that of during HIPIB treatment either a few times.

2. Experiment

The phase composition of the samples was investigated using X-ray diffraction analysis (XRD) in the Bragg–Brentano geometry, with a CuK_α radiation. The surface and cross-section morphology, the concentration distribution of elements was studied by scanning electron microscopy (SEM) and energy-dispersive X-ray analysis (EDXA). Microhardness of the samples was tested by means of a PMT-3 microhardmeter with a Vickers indentor under the load ranging from 1 to 2N.

Samples of WC–TiC–Co hard alloy (T15K6) had the following averaged element composition: W – 46 at %, Ti – 12 at %, Co – 5 at %., C – 37 at %. The phase composition of alloy after sintering includes the following main phases: WC, (Ti, W)C, Co (Fig. 1, *a*).

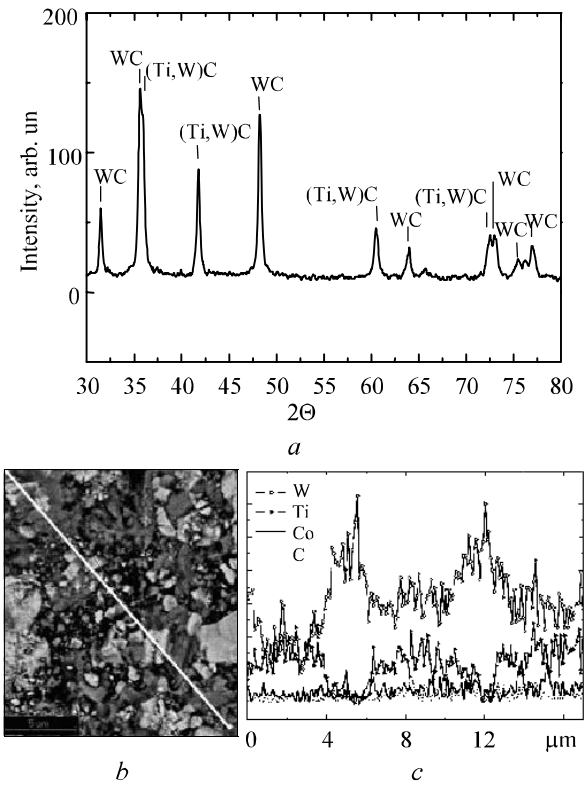

Fig. 1. XRD patterns of hard alloy T15K6 (*a*), surface structure (*b*), EDXA distribution of elements along a line on the surface (*c*)

SEM and EDX dates show that the very light faceted grains belong WC, gray grains belong solid state (Ti, W)C. Co and C distribute along carbide grains. Hardness of alloy was (13 ± 2) GPa.

Condition of HIPIB treatments was: the ion energy – 320 kV, the ion current density – 100 A/cm^2 the pulse duration – 70–100 ns, the incident energy density – 7 J/cm^2 during impulse, the number of impulses – three.

The gas discharge magnetoplasma compressor used for generating CPF was described in details in [5]. The experiments were performed in a 'residual gas' mode during which the vacuum chamber was filled with nitrogen. The pulse duration was 100 μs. Two types of experiments were carried out to study the influence of the treatment parameters on phase composition, microstructure and properties alloy surface layer. In the first experiment, the distance between target and cathode was 8 cm for first type of experiments and 14 cm for second. The treatment of samples was made with five impulses. Absorbed energy density was accordingly ~ 40 and 13 J/cm^2 during impulse [5, 6].

3. Results

As a result of HPIB action with the energy density of 7 J/cm^2 on hard alloy T15K6 there is the melting of its surface on the depth of a several micron (Fig. 2).

The surface roughness of hard alloy increases. It is observed the partial fusion of carbide grains – (Ti, W)C and WC (Fig. 2, *a*), that is confirmed by EDXA distribution of elements along a line on Fig. 2, a (Fig. 2, *b*). The layer of ~ 10 microns in depth with high density of defects in the form of cracks in carbides and pores (heat affected zone) is followed by the melted layer (Figs. 2, *c* and *d*).

The partial fusion of carbides is confirmed also by the redistribution of intensities between diffraction lines corresponding to WC and (Ti, W)C (Fig. 3).

The intensity of diffraction line of carbide (Ti, W)C increases and diffraction line is shifted to the greater diffraction angles. The lattice parameter of solid solution (Ti, W)C before and after HPIB action was determined from the X-ray diffraction patterns obtained by the precision analysis with the big exposition and small angle increment, that provided the lattice parameter error of $5 \cdot 10^{-5}$ nm (Table 1).

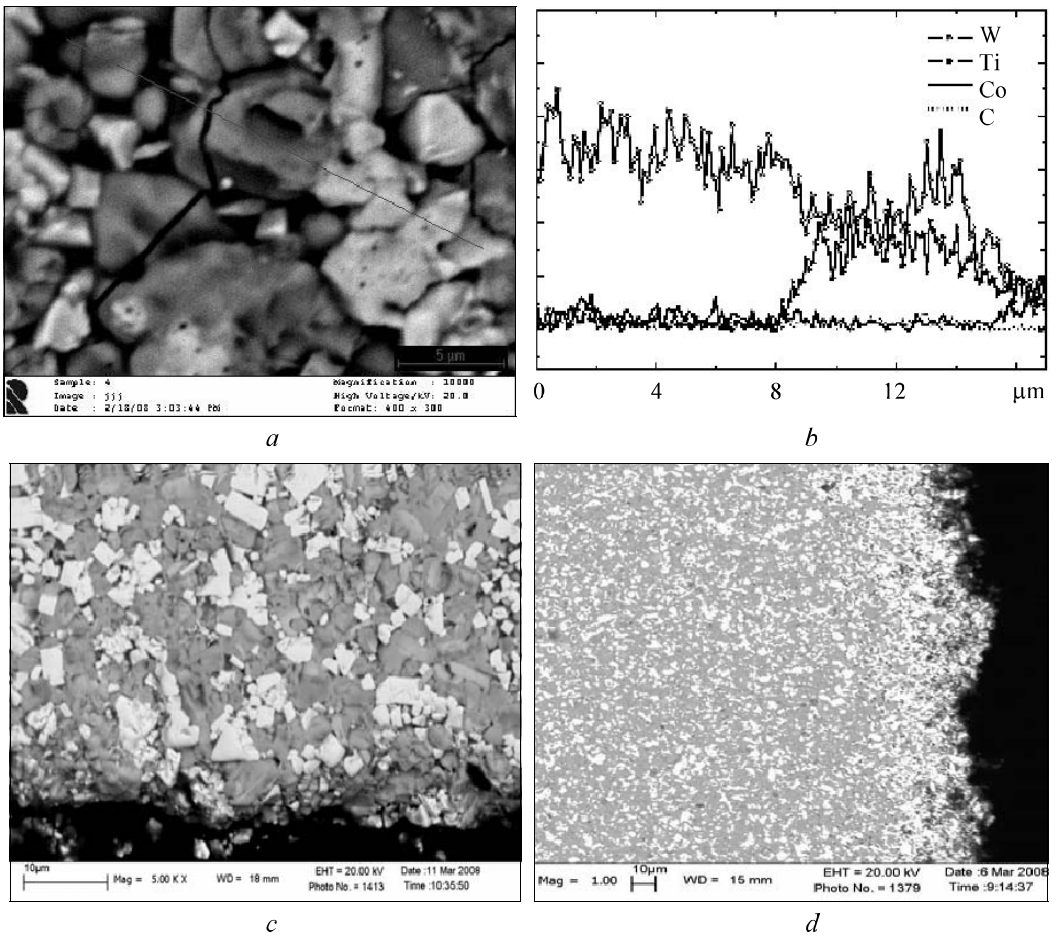

a *b* *c* *d*

Fig. 2. Surface structure (*a*), EDXA distribution of elements along a line on the surface (*b*), changing of cross section structure (obtained at the different magnification) (*c*), (*d*) of hard alloy T15K6 after HPIB action with the energy density of 7 J/cm^2

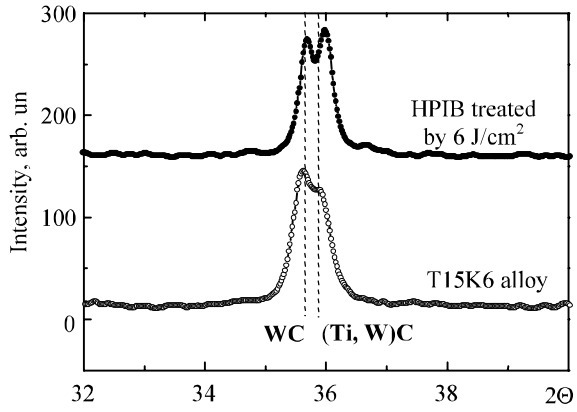

Fig. 3. XRD patterns of hard alloy T15K6 after HPIB action with the energy density of 7 J/cm^2

Table 1. Lattice parameter of solid solution (Ti, W)C of alloy T15K6 after treatment by HPIB and CPF

Treatment type	Lattice parameter of solid solution (Ti, W)C, nm
Untreated T15K6	0.4325
HPIB_7 J/cm^2	0.4319
CPF_13 J/cm^2	0.4315
CPF_40 J/cm^2	0.4300

As it is known from the literature, at the thermodynamic balance the lattice parameter of solid solution (Ti, W)C decreases with the growth of the tungsten content. At the ratio 1WC:1TiC lattice parameter can have the minimum value of 0.4322 nm [7].

Decrease of lattice parameter after HPIB action is a consequence of smaller nuclear radius of tungsten in comparison with the titanium (W – 0.141 nm; Ti – 0.149 nm). Thus, after HPIB action on the hard alloy in the surface layer there is a formation of solid solution (W, Ti)C more saturated with tungsten.

In the case of CPF treatment on hard alloy with energy density of 13 and 40 /cm^2 in pulse there is a melting of surface layer of an alloy. With the growth of energy density of CPF treatment the thickness of the melted layer increases on the average from several micron to 10 microns (Figs. 4, 5).

In the melted layer concentration of tungsten exceeds concentration of the titanium. With the increase in energy density of treatment the tungsten content increases in the melted layer (Figs. 4, 5). This is confirmed both by the XRD data and by the results of calculation of lattice parameter of the solid solution (Fig. 6, Table 1). It is necessary to notice that asymmetrical double diffraction peak of a solid solution is due to the occurrence of doubling of X-ray copper radiation consisting from $CuK_{\alpha 1}$ and $CuK_{\alpha 2}$.

The size of pores and cracks present at the melted layer exceeds the sizes of similar defects at HPIB action and reaches a share of micron for pores and the micron sizes for cracks. Cracks and pores are formed

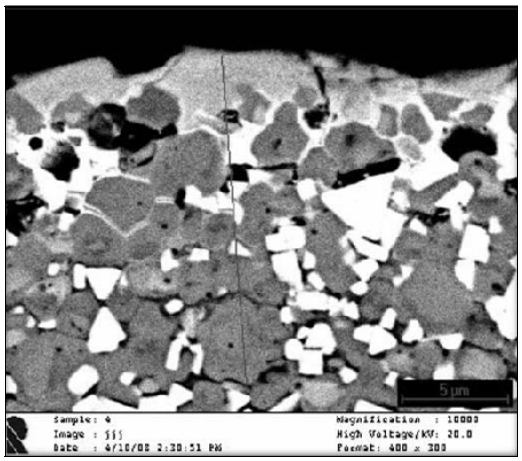

a

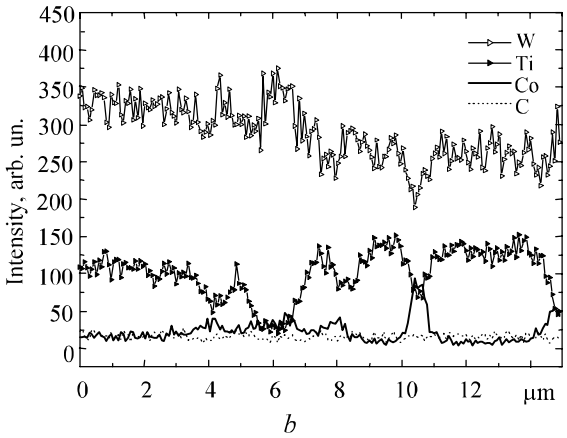

b

Fig. 4. Changing of cross section structure (*a*) and EDXA distribution of elements along a lines on the cross section of hard alloy T15K6 (*b*) after CPF treatment with the energy density of 13 J/cm^2

as a result of ultra-fast crystallization because of a significant difference of heat-transfer properties of Co and carbides of hard alloy [8]. The thicker layer with the changed microstructure forms after the melted layer. The characteristic feature of this layer is the increase in relative concentration of tungsten at the carbides grains boundaries. In the SEM images of cross-section structure (Figs. 4, 5), the boundaries along grey grains of (Ti, W)C have more light view because of enrichment by tungsten.

It is a layer of contact melting of interphase boundaries of carbides grains and binding cobalt. The more close to the surface, the more thickness of a layer of contact melting and is less the size of initial solid solution carbides grains. Lower temperature of WC melting (3058 °C) in comparison with TiC (3290 °C) causes saturation of interphase zones first of all by tungsten. It is necessary to note the formation in the melted layer of cellular element contrast on all its thickness. The size of cells does not exceed 0.5 microns.

Results of hardness measurement presented in Fig. 7 testify that at the both HPIB and CPF treatment hardness of surface layer of hard alloy increases.

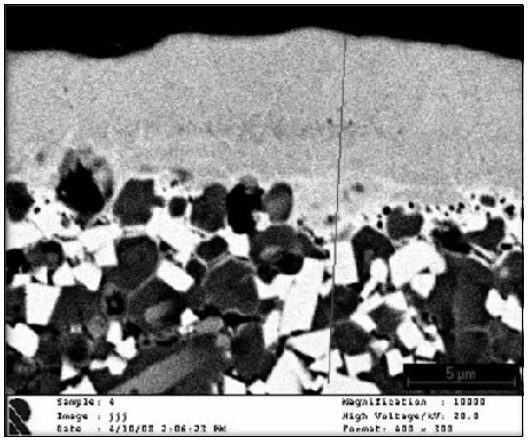

a

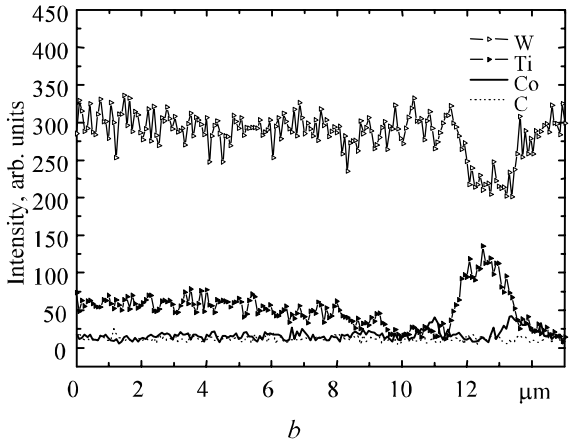

b

Fig. 5. Changing of cross section structure (*a*) and EDXA distribution of elements along a lines on the cross section of hard alloy T15K6 (*b*) after CPF treatment with the energy density of 40 J/cm^2

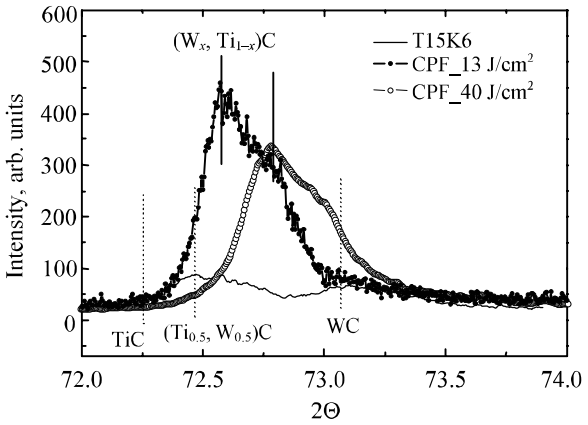

Fig. 6. Areas of XRD patterns of hard alloy T15K6 before and after CPF treatment

The maximum increase in hardness of an alloy in 2 times is reached at CPF treatment.

4. Conclusions

At HPIB and CPF treatment of hard alloy T15K6 with approximate energy densities greater pulse duration

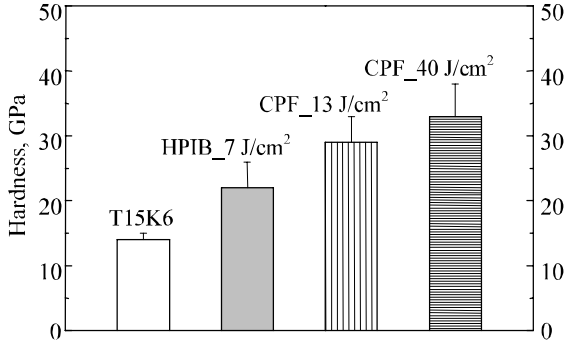

Fig. 7. Hardness of hard alloy T15K6 before and after HPIB and CPF treatment

of CPF results in more intensive fusion of carbides of tungsten and a solid solution and in the formation of a continuous surface layer of a solid solution $(W_x, Ti_{1-x})C$ supersaturated by tungsten. The increase in energy density of CPF treatment results in the increase in its thickness (~ 10 microns) and degree of its supersaturation by tungsten. Behind the melted layer the layer (~ 10 microns in thickness) containing interlayers of the solidified liquid phase as a result of contact melting of interphase boundaries of grains of carbides and cobalt is formed. In the case of HPIB action behind the melted layer the extended layer (up to 10 microns) with high density of bulk defects (pores, cracks) is formed. Moreover, the size of this defect is smaller in comparison with its after CPF treatment. Hardness of the surface layer containing supersaturated solid solution $(W_x, Ti_{1-x})C$ in some micron in the thickness exceeds in 2 times the hardness of untreated hard alloy T15K6.

References

[1] A.D. Korotaev, A.N. Tsyumentsev, Yu.P. Pinzhin, and G.E. Remnev, Surface and Coatings Technol. **185**, 38 (2004).

[2] G.E. Remnev and V.A. Tarbokov, IEEJ Trans. **124**/6, 76 (2004).

[3] Y.F. Ivanov, V.P. Rotshtein, D.I. Proskurovsky, P.V. Orlov, K.N. Polestchenko, G.E. Ozur, and I.M. Goncharenko, Surface and Coatings Technol. **125**, 251 (2000).

[4] G. Mueller, V. Engelko, A. Weisenburger, and A. Heinzel, Vacuum **77**, 469 (2005).

[5] V.V. Uglov, V.M. Anishchik, V.M. Astashinski, N. N. Cherenda, L.G. Gimro, and A.V. Kovyaza, Surface & Coatings Technol. **200**, 249 (2005).

[6] N.N. Cherenda, V.V. Uglov, V.M. Anishchik, A..K. Stalmashonak, V.M. Astashinski, A.M. Kuzmickii, A.V. Punko, G. Thorwath, and B. Stritzker, Surface & Coatings Technol. **200**, Issue 18–19, 5334 (2006).

[7] M.J. Mas-Guindal, L. Contreras, X. Turrillas, G.B.M. Vaughan, A. Kvick, and M.A. Rodrəguez, J. of Alloys and Compounds **419**, 227 (2006).

[8] K.H. Lee, S.I. Cha, B.K. Kim, and S.H. Hong, Int. J. of Refractory Met. and Hard Mat. **24**, 110 (2006).